Load-Modulating Loop Combiner for Linear Power Amplification

William Sear[®], Member, IEEE, and Taylor W. Barton[®], Senior Member, IEEE

Abstract—This work presents a novel power amplifier (PA) architecture employing a feedforward-like loop structure for the linearization of a load-modulated PA. The load-modulating loop combiner (LMLC) is related to a feedforward amplifier, but with the interaction between the main and auxiliary amplifiers to generate both distortion cancellation and load modulation. A brief overview of the underlying theory is presented, followed by a hardware demonstrator operating at 3.5 GHz with 42-dBm peak output power and 55% peak drain efficiency in CW. When excited by a 100-MHz LTE signal, it maintains a 3-ppt EVM improvement and a 2–5-ppt average drain efficiency improvement compared to its standalone main amplifier.

Index Terms—5G mobile communication, distortion reduction, efficiency enhancement, feedforward, power amplifiers (PAs).

I. INTRODUCTION

THE feedforward architecture (FFA) was originally developed in 1923 as a way to reduce distortion in power amplifiers (PAs) [1]. This approach employs an auxiliary PA to cancel the distortion products generated by the main amplifying PA, through the use of two loops. In the first loop, the distortion generated by the main PA is detected by subtracting from its output signal an attenuated version of the desired signal. Then, this distortion signal is amplified and added to the PA output through the appropriate amplitude and phase transfer function. Since the invention of this technique, the two loops have been almost exclusively implemented using directional couplers, that is, without feedback interaction between the injected feedforward signal and the main PA. Indeed, the FFA predates the development and popularization of feedback techniques for linearization.

The FFA has a superficial resemblance to that of the Doherty PA (DPA) [2], [3], [4], [5], [6], except that the DPA employs a feedback-like interaction between the main and auxiliary PAs to produce load modulation. Variations of the DPA using a distortion product cancellation strategy analogous to that in an FFA have been proposed, including tuning the main and auxiliary PA intermodulation distortion (IMD) products to cancel at the output [2], or introducing nonlinearities in a driver amplifier to generate canceling distortion effects [3]. These methods focus on canceling IMD terms, effectively operating as the second "loop" in the FFA. Other works have combined the feedforward and DPA architectures by replacing

Manuscript received 2 August 2022; revised 8 September 2022; accepted 28 September 2022. This work was supported by the National Science Foundation under Grant 1846507. (Corresponding author: William Sear.)

The authors are with the Department of Electrical, Computer, and Energy Engineering, University of Colorado at Boulder, Boulder, CO 80309 USA (e-mail: william.sear@colorado.edu; taylor.w.barton@colorado.edu).

Color versions of one or more figures in this letter are available at https://doi.org/10.1109/LMWC.2022.3211162.

Digital Object Identifier 10.1109/LMWC.2022.3211162

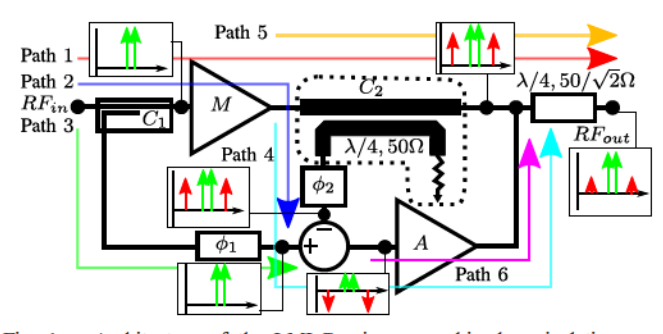


Fig. 1. Architecture of the LMLC using a combined nonisolating combiner/coupled line coupler structure. Also shown are various critical signal paths through the architecture relevant to load modulation (paths 1–3 and 6) and distortion cancellation (paths 4 and 5). At select points, the fundamental (green) and distortion (red) tones are shown.

the main PA of the FFA with a DPA, having the correction signal injected either through a coupler as in a standard feedforward amplifier (e.g., [7]), or serving as a third input to the DPA combining node [8]. This category of approaches can be generalized as improving the FFA efficiency by using a more efficient main PA.

In this work, we present the novel load-modulated loop combiner (LMLC) PA architecture, shown in the block diagram form in Fig. 1. The LMLC draws from the FFA in that it has a dual-loop structure, but with a nondirectional summing junction at the output stage. Similar to [8], the auxiliary PA operates on the fundamental signal component in addition to the distortion products, but in the LMLC, a single auxiliary PA simultaneously provides load modulation and distortion cancellation functions. Compared to linear DPA techniques [5], an advantage of the LMLC approach is that the distortion reduction can be controlled via the input coupler design, rather than requiring extensive modeling of the nonlinear PA behaviors.

II. LMLC ARCHITECTURE

The LMLC is designed to operate with the typical DPA load modulation, that is, the nonisolating output combiner is designed based on a quarter wavelength line with offset lines and the fundamental-frequency operation follows standard DPA theory that will not be reproduced here. The need to correctly design and drive the auxiliary amplifier to produce both load modulation and feedforward cancellation presents the most significant challenge to the LMLC architecture. In this theory discussion, each block x in Fig. 1 is described in terms of their through gain A_x , coupled gain C_x (if appropriate), and phase shift θ_x . To control the behavior of the fundamental signal and distortion products simultaneously, the LMLC comprises four tuning elements: delay lines ϕ_1 , ϕ_2 (with phase shifts denoted θ_{ϕ_1} , θ_{ϕ_2}) and the coupling factors of couplers C_1 , C_2 (C_{C_1} , C_{C_2}). These elements are chosen to

1531-1309 © 2022 IEEE. Personal use is permitted, but republication/redistribution requires IEEE permission. See https://www.ieee.org/publications/rights/index.html for more information.

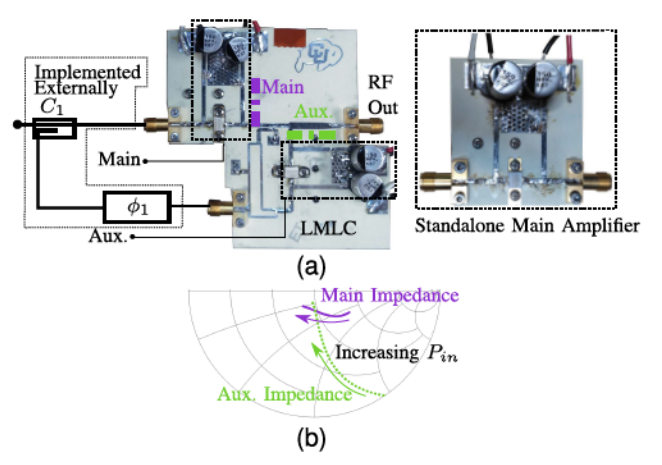


Fig. 2. (a) Photographs of the fabricated proof-of-concept 3.5-GHz LMLC PA measuring 3.3×3.3 in and the standalone main amplifier measuring 1.6×1.7 in. The two RF inputs are driven with a constant relative amplitude and phase shift to realize C_1 and $\theta_{\phi 1}$. (b) Smith chart plots simulated load modulation trajectories for the LMLC reference planes shown in (a).

control the response through the six signal paths shown in Fig. 1 such that paths 4 and 5 are equal in amplitude and opposite in phase to maximize distortion cancellation and the vector sum of paths 2 and 3 plus path 4 has equal phase delay to path 1 to produce load modulation. Paths 1 and 2 must also be selected such that the amplitude of the fundamental signal arriving at the input of the auxiliary amplifier changes correctly with the input signal for load modulation.

The delay θ_{ϕ_2} and coupling factor C_{C_2} directly control path 4, which must be adjusted to have equal amplitude and 180° phase difference from path 3 in order to cancel the distortion products generated by the main amplifier at the output. To match the amplitude of these two paths, C_{C_2} must be selected in terms of the gains of the through the path of the coupler (A_{C_2}) , the delay line ϕ_1 (A_{ϕ_1}) , and the auxiliary amplifier (A_A) as

$$C_{C_2} = \frac{A_{C_2}}{A_A A_{\phi_1}}. (1)$$

In (1), the gain A_{ϕ_1} can be approximated as 1, which means that the coupling factor C_{C_2} should be selected to be approximately equivalent to the gain of the auxiliary amplifier. This selection of the coupling factor C_{C_2} is consistent with how it is selected in the conventional FFA.

Delay θ_{ϕ_2} is selected such that paths 4 and 5 are 180° out of phase from each other, again to ensure cancellation. Assuming that the subtractor element is ideal, this results in the following requirement for θ_{ϕ_2} :

$$\theta_{\phi_2} = (\theta_{A_{C_2}} - \theta_{C_{C_2}}) - \theta_A. \tag{2}$$

We note that the selection of θ_{ϕ_2} and C_{C_2} also perturbs the fundamental signal component presented to the auxiliary amplifier, which will adversely affect the load modulation. Conveniently, θ_{ϕ_1} and C_{C_1} only affect the fundamental signal component and can be selected so that the correct fundamental signal drives the amplifier. We will select the coupling factor C_{C_1} and phase delay θ_{ϕ_1} such that the magnitude of the fundamental signal applied to the input of the auxiliary amplifier is an appropriately scaled copy of the input signal. At the fundamental frequency, the input signal to the auxiliary amplifier is the vector sum of the signals from paths 2 and 3, so both the amplitude and phase of both signal paths control the overall amplitude and phase of the input signal to the auxiliary amplifier. Here, we remove the combined amplitude

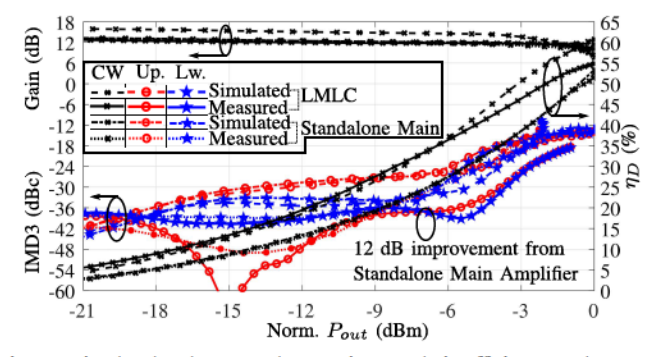


Fig. 3. Simulated and measured CW gain, CW drain efficiency, and 10-MHz IMD3 response of the LMLC and its standalone main amplifier centered at 3.5 GHz. The LMLC reaches a peak CW output power of 42 dBm, and the standalone main amplifier has a peak CW output power of 40 dBm.

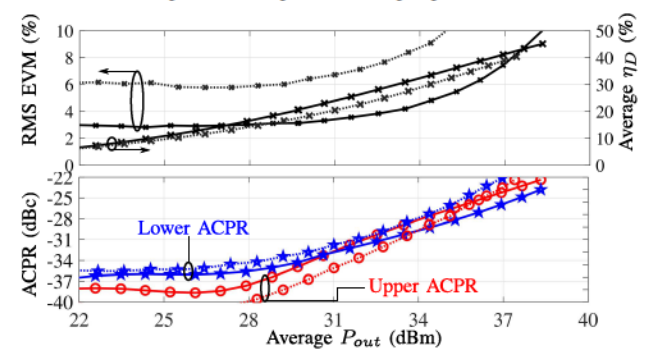


Fig. 4. Measured rms EVM, average drain efficiency, and ACPR of the LMLC (solid) and standalone main amplifier (dotted) when they are excited by a 100-MHz-wide LTE-like signal with 10-dB PAPR. Measurements include the performance of the RFLUPA02G06GC driver amplifier for both the LMLC and standalone main amplifier.

and phase dependence by setting the phase through paths 2 and 3 plus the additional delay in path 6 to be equal to the delay in path 1, such that the fundamental signals through the main and auxiliary amplifier are correctly phase aligned so that load modulation occurs. This condition is met when the phase delays through paths 2 and 3 are equal [a consequence of the previous selection of θ_{ϕ_2} in (2)] resulting in the following requirement for θ_{ϕ_1} :

$$\theta_{\phi_1} = (\theta_{A_{C_1}} - \theta_{C_{C_1}}) + (\theta_M - \theta_A) + \theta_{A_{C_2}}.$$
 (3)

With the phase delay θ_{ϕ_1} determined from (3), we finally select the coupling factor C_{C_1} so that the fundamental signal presented to the input of the auxiliary is a copy of the input being presented to the main, leading to the condition

$$C_{C_1} = \pm \frac{(A_M C_{C_2} A_{\phi_2})^2 + 1}{\sqrt{(A_M C_{C_2} A_{\phi_2})^4 + 6(A_M C_{C_2} A_{\phi_2})^2 + 1}}.$$
 (4)

The expression in (4) at first appears to be complicated, but assuming the loss of delay line ϕ_2 (A_{ϕ_2}) is small and that the gain of the main amplifier (A_M) and coupling factor of C_2 are equal and opposite in magnitude (a condition met when $A_M \approx A_A$), the coupling factor C_{C_1} simplifies to around 6 dB, half the coupling of a conventional DPA architecture.

III. DESIGN OF A 3.5-GHZ PROTOTYPE AMPLIFIER

The 3.5-GHz prototype design uses identical main and auxiliary PA networks based on the CG2H40010 device from Wolfspeed. The auxiliary amplifier is biased into class-C, while the main amplifier operates in deep class-AB; similar to conventional DPA designs, this bias selection trades off efficiency and linearity [4]. Under these biasing conditions, the LMLC design constraint from (4) that $A_M \approx A_A$ is

TABLE I
PERFORMANCE SUMMARY AND COMPARISON TO STATE-OF-THE-ART FFA
AND DPAs AT SIMILAR FREQUENCY AND OUTPUT POWER

| Reference | [5] | [10] | [6] | [11] | This Work |
|---|---------|--------|-------|-------|--------------|
| Device Technology | † | • | † | ‡ | ‡‡ |
| Architecture | DPA | FFA | DPA | QDPA | LMLC |
| Freq. (GHz) | 3.5 | 3.5 | 3.5 | 3.5 | 3.5 |
| Max. Pout (dBm) | 41* | 30.8 | 40* | 42* | 42 |
| Max. η_D /PAE (%) | 70*/60* | -/27.2 | -/51* | 70/- | 55/50 |
| -6dB OBO η _D /PAE (%) | 58*/48* | -/10* | -/36* | 50*/- | 41/35 |
| $\eta_{D,\text{avg}}/\text{PAE}_{\text{avg}}$ (%)\$ | 65*/58* | -/10* | -/20* | 55*/- | 48/41 |
| Poutavg (dBm)\$ | 38* | 25* | 27* | 36* | 38 |
| Tone spacing (MHz)\$ | 5 | 10 | 5 | 10 | 10 |

- - not reported; * - read from graph; \$ - reported for IMD3 of -30 dBc † - CGH40006P; ‡ - CGH40008P; ‡‡ - CG2H40010F; ◊ - HMC327

satisfied after the auxiliary amplifier has turned on, and the main amplifier has begun to compress, corresponding to the region where distortion reduction will be most valuable.

The coupler C_2 and the 50- Ω $\lambda/4$ section of the Doherty combiner can be conveniently combined into a single coupled line coupler structure as shown in Fig. 1 because the coupled-line coupler has a through phase delay of $\lambda/4$. In our implementation, the coupled line segment is shorter than $\lambda/4$ for practical considerations of the interconnection with the auxiliary amplifier while maintaining the correct through a phase shift, and the coupler is designed to have a coupling factor of 15 dB [to compensate for the gain expected from the main amplifier following (1)]. Finally, the subtractor element is implemented as a rat-race combiner whose size is optimized to connect the input of the auxiliary amplifier and output of the coupled-line coupler with the appropriate phase delay. In our experimental setup, the coupler C_1 and phase delay element ϕ_1 are implemented using a connectorized 6-dB coupler and analog phase shifter to allow for tuning, although no deviation from the theoretical values was necessary. In a future realization, the fixed amplitude/phase relationship between the two inputs is straightforward to implement using a passive structure. The final LMLC and standalone main PA as fabricated can be seen in Fig. 2 with the realized load modulation trajectories for the main and auxiliary LMLC PAs.

IV. MEASURED RESULTS

The LMLC prototype and standalone main PA are measured using the test setup described in Section III under CW, twotone, and modulated signal excitations. With $C_{C_1} = 6$ dB and $\theta_{\phi_1} = 330^{\circ}$, the simulated and measured CW gain, CW drain efficiency (η_D), and 10-MHz two-tone IMD3 are captured in Fig. 3. The general response of the LMLC for both the measured CW and two-tone responses is consistent with the simulated performance, although the measured drain efficiency is lower than simulated at high output power, likely due to the turn-on characteristics of the auxiliary PA. The measured 10-MHz IMD3 of the LMLC is 3–30 dB lower than simulated, most likely due to onboard tuning of the IF impedance presented to the drain of the main PA [9]. The feedforward action is evident when compared to the standalone main PA above 9-dB back-off from peak output power, although the standalone main has lower peak efficiency than the LMLC because it is not optimized for a 50- Ω output termination.

We can see in Fig. 4 that when excited by a 10-dB peak-to-average power ratio (PAPR) 100-MHz LTE-like signal, the LMLC maintains an rms EVM below 3% until 28 dBm average output power, while the adjacent channel power ratio (ACPR) remains below -35 dBc with a 17% average drain

efficiency. This is an improvement over the standalone main amplifier reported here and the DPA reported in [6], which reaches -35 dBc ACPR at 24 dBm average output power for a 5-MHz-wide LTE signal.

A comparison of these measured results to state-of-the-art linear-efficient DPAs and FFAs at a similar frequency and output power is shown in Table I. In CW measurement, the LMLC performs comparably to the DPAs, where we note that the LMLC has a slightly lower PAE but 2-dB higher output power. The LMLC's strength is in its linearity-efficiency tradeoff; as an approximate means to compare these works, the table includes the PAE and output power at the first (lowest) output power for which the IMD3 response to a two-tone test reaches -30 dBc, along with the tone spacing at which this measurement is reported. At 10-MHz tone spacing, the LMLC provides 11 dB greater output power than [4] with a similar PAE. Compared to the excellent work in [5], the difference between the peak and average two-tone PAE is similar for the two designs. We also note that the LMLC's IMD3 is substantially lower over a wide power range compared to [5], for example, reaching a -35-dBc IMD3 at 36 dBm/35% PAE compared to 19 dBm/10% in [5].

V. Conclusion

The novel LMLC architecture draws from the FFA and DPA techniques to simultaneously produce load modulation and distortion product cancellation. A proof-of-concept first-pass design performs on par or better than the SOTA in terms of both efficiency and linearity, without DPD. A complete design methodology is presented and validated that enables systematic linear-efficient PA design without requiring extensive modeling or optimization of nonlinear PA behaviors.

REFERENCES

- A. Katz, J. Wood, and D. Chokola, "The evolution of PA linearization: From classic feedforward and feedback through analog and digital predistortion," *IEEE Microw. Mag.*, vol. 17, no. 2, pp. 32–40, Feb. 2016.
- [2] C. Musolff, M. Kamper, Z. Abou-Chahine, and G. Fischer, "Linear and efficient Doherty PA revisited," *IEEE Microw. Mag.*, vol. 15, no. 1, pp. 73–79, Jan. 2014.
- [3] R. Giofrè and P. Colantonio, "A high efficiency and low distortion 6 W GaN MMIC Doherty amplifier for 7 GHz radio links," *IEEE Microw. Wireless Compon. Lett.*, vol. 27, no. 1, pp. 70–72, Jan. 2017.
- [4] Y. Cho, D. Kang, J. Kim, K. Moon, B. Park, and B. Kim, "Linear Doherty power amplifier with an enhanced back-off efficiency mode for handset applications," *IEEE Trans. Microw. Theory Techn.*, vol. 62, no. 3, pp. 567–578, Mar. 2014.
- [5] C. Musolff, M. Kamper, Z. Abou-Chahine, and G. Fischer, "A linear and efficient Doherty PA at 3.5 GHz," *IEEE Microw. Mag.*, vol. 14, no. 1, pp. 95–101, Jan./Feb. 2013.
- [6] W. Hallberg, P. E. de Falco, M. Ozen, C. Fager, Z. Popovic, and T. Barton, "Characterization of linear power amplifiers for LTE applications," in *Proc. IEEE Top. Conf. RF/Microw. Power Modeling Radio* Wireless Appl. (PAWR), Jan. 2018, pp. 32–34.
- [7] R. N. Braithwaite, "A comparison for a Doherty power amplifier linearized using digital predistortion and feedforward compensation," in *IEEE MTT-S Int. Microw. Symp. Dig.*, May 2015, pp. 1–4.
- [8] Y. Hu and S. Boumaiza, "Doherty power amplifier distortion correction using an RF linearization amplifier," *IEEE Trans. Microw. Theory Techn.*, vol. 66, no. 5, pp. 2246–2257, May 2018.
- [9] W. Sear, D. T. Donahue, M. Pirrone, and T. W. Barton, "Bias and bias line effects on wideband RF power amplifier performance," in Proc. IEEE 22nd Annu. Wireless Microw. Technol. Conf. (WAMICON), Apr. 2022, pp. 1–4.
- [10] M. Jung, S. Min, and B.-W. Min, "A quasi-balanced power amplifier with feedforward linearization," *IEEE Microw. Wireless Compon. Lett.*, vol. 32, no. 4, pp. 312–315, Apr. 2021.
- [11] H. Lyu, Y. Cao, and K. Chen, "Linearity-enhanced quasi-balanced Doherty power amplifier with mismatch resilience through series/parallel reconfiguration for massive MIMO," *IEEE Trans. Microw. Theory Techn.*, vol. 69, no. 4, pp. 2319–2335, Apr. 2021.